Smoothing and Interpolation of In-Vivo B_{1+} Images

A. Petrovic[1,2], Y. Dong[3], S. Keeling[3], and R. Stollberger[1]
[1]Institute of Medical Engineering, University of Technology Graz, Graz, Austria, [2]Ludwig Boltzmann Institute for Clinical Forensic Imaging, Graz, Austria, Austria, [3]University of Graz

Introduction and Purpose

Magnetic resonance imaging at high field strengths (≥ 1.5T) suffers from perturbations caused by the inhomogeneity of the RF excitation field B_{1+} within the human body. These inhomogeneities are especially critical for quantitative MR measurements. Measurements of the active RF field can be used to correct for these inhomogeneities [1]. However, in-vivo measurements of these fields are prone to artifacts from cavities, bone-tissue interfaces, physiological motions and flow. To correct for these artifacts dedicated image processing algorithms must be applied. Since the expected B_{1+} field is a smoothly varying function, the correct smoothing and interpolation of the B_{1+}-images is necessary. In the recent literature, simple Gaussian filtering and polynomial fitting were described in order to smooth and interpolate the measured images [2, 3, 4, 5]. In this work, a new variational approach for smoothing was applied, and the performance was compared to that of outlier insensitive median filtering. The application of these methods on the correction of T1 times in DCE images results in considerable improvement.

Theory and Methods

The new variational approach that was used is given by eqn. 1, where g is the measured image; $\hat{g}$ is the reconstructed image, μ the regularization parameter and Ω the image domain. The function γ(g) works as an outlier detection, being zero for values of g that cannot be trusted, and one otherwise. The parameter q determines the data fidelity term to be either the L_2 or L_1 norm. The regularization term was chosen to be the L_2 norm of the second order derivatives of $\hat{g}$, in order to put a constraint on the smoothness of the function. Solving the minimization problem in eqn. 1 leads to the following partial differential equations (eqn. 2 for L_2 data term, eqn. 3 for L_1 data term). The corrected image $\hat{g}$ corresponds to the active excitation field, and thus to the actual flip angle at every position in the body. The variational formulation was minimized by using a conjugate gradient solver [6]. The outlier detection function γ was implemented as follows: the perturbed image was filtered with a median and a Gaussian filter, then the median filtered image was subtract from the other, and a thresholding function was applied to detect outliers. This procedure generates an image mask for subsequent smoothing and interpolation. The choice of the filter parameters was performed manually for typical B_1-images (median kernel 30x30, Gaussian kernel 5x5, sigma=1.5).

$$\min\left\{J(\hat{g}) = \int_{\Omega} \gamma(g)\,|\,\hat{g}-g\,|^{q}\,dx + \frac{\mu}{2}\int_{\Omega} |\Delta\hat{g}\,|^{2}\,dx\right\}, \quad q \in \{1,\,2\}, \tag{1}$$

$$\mu\Delta^2\hat{g} + \gamma(g)(\hat{g}-g) = 0 \tag{2}$$

$$\mu\Delta^2\hat{g} + \gamma(g)\frac{\hat{g}-g}{|\,\hat{g}-g\,|} = 0 \tag{3}$$

The optimal smoothing parameters were obtained by minimizing the RMSE of the original minus the smoothed image for test datasets. For the choice of the optimal parameters for in-vivo data the residual had to equal the estimated noise variance, whereas the exclusion of the outliers was considered first.

Test datasets differing in artifact modality and noise level, were created based on statistical properties of real B_{1+}-images. After generation they were split into training and a test set, smoothed, and finally the outcome was assessed in terms of accuracy and precision. Validation was also performed by the use of original images and visual inspection of the outcome.

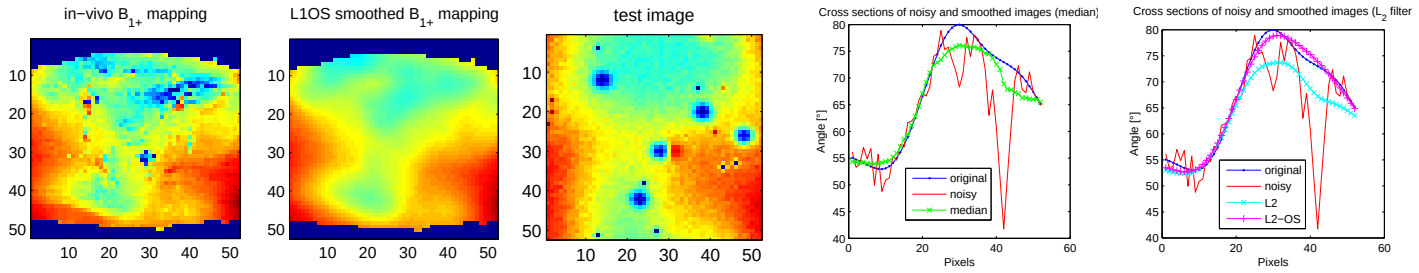

(a) (b) (c) (d) (e) (f)

Fig. 1.: (a) shows an example of a strongly perturbed B_1-image from the abdominal region, (b) is the same image smoothed with the L_1 filter with outlier suppression, (c) is an example of a rather noisy test image with blob-like artifacts , (d) to (f) are examples of a cross section of the original, noisy and smoothed images in degrees, for the median filter (d), the variational approach with L_2 data norm (e), and the variational approach with L_1 norm (f). OS denotes outlier suppression.

Results and Conclusion

Fig. 1 shows an in-vivo B_{1+}-image (a) and a smoothed version of it (b). Fig 1(c) is an example of a test image set corrupted by blob-like artifacts and additive Gaussian noise. The performance of the different smoothing algorithms depended on the test image set. Outlier suppression could improve the results in all cases. For images as in fig. 1(c) the variational approaches with outlier suppression performed best in terms of accuracy and precision producing an overall median RMSE (median of the RMSE of smoothed minus original image, for 150 test images) of about 2%. The pure L_1 approach yielded a median RMSE 2.2%, still being better than the median filter with 2.7%. The pure L_2 approach seems to be strongly attracted by the hole-like artifacts and performed worst with a median RMSE of 3.6%. Compared to preliminary simulations using a simple thresholding scheme for outlier detection, the median value of the RMSE could be improved by 10 to 20 %. The smoothing of original B_{1+}-images points out that the choice of the regularization parameters and the size of the filter kernel is crucial. Visual inspection after the smoothing process is therefore recommended for new datasets. It was also found that the variational approach largely avoids steps in contrast to the median filter, and thus produces results that are physically likely. This can be seen in the cross sections displayed in figs. 1(d) to (f), in which also the dominance of the L_1 approach (d) is clearly visible.

References

[1] R. Stollberger et al., Proc. ISMRM 16, 3091 (2008). [2] G. Helms et al., MRM 60:739-743 (2008). [3] R. Treier et al., MRM 57:568-576 (2007). [4] C. C. Guclu et al., Proc. ISMRM 14, 753, (2006). [5] G W Miller et al., MAGMA 16: 218–226 (2004). [6] S.L. Keeling et al., Applied Mathematics and Computation 158(2): 53–82 (2004).